Molecular Properties of Purified Human Uncoupling Protein 2 Refolded From Bacterial Inclusion Bodies

Mika B. Jekabsons,[1,2,3] Karim S. Echtay,[1] Ignacio Arechaga,[1] and Martin D. Brand[1]

One way to study low-abundance mammalian mitochondrial carriers is by ectopically expressing them as bacterial inclusion bodies. Problems encountered with this approach include protein refolding, homogeneity, and stability. In this study, we investigated protein refolding and homogeneity properties of inclusion body human uncoupling protein 2 (UCP2). *N*-methylanthraniloyl-tagged ATP (Mant-ATP) experiments indicated two independent inclusion body UCP2 binding sites with dissociation constants (K_d) of 0.3–0.5 and 23–92 μM. Dimethylanthranilate, the fluorescent tag without nucleotide, bound with a K_d of greater than 100 μM, suggesting that the low affinity site reflected binding of the tag. By direct titration, UCP2 bound [8-^{14}C] ATP and [8-^{14}C] ADP with K_ds of 4–5 and 16–18 μM, respectively. Mg^{2+} (2 mM) reduced the apparent ATP affinity to 53 μM, an effect entirely explained by chelation of ATP; with Mg^{2+}, K_d using calculated free ATP was 3 μM. A combination of gel filtration, Cu^{2+}-phenanthroline cross-linking, and ultracentrifugation indicated that 75–80% of UCP2 was in a monodisperse, 197 kDa form while the remainder was aggregated. We conclude that (a) Mant-tagged nucleotides are useful fluorescent probes with isolated UCP2 when used with dimethylanthranilate controls; (b) UCP2 binds Mg^{2+}-free nucleotides: the K_d for ATP is about 3–5 μM and for Mant-ATP it is about 10 times lower; and (c) in $C_{12}E_9$ detergent, the monodisperse protein may be in dimeric form.

KEY WORDS: UCP2; mitochondrial carrier; hydroxyapatite; fluorescence resonance energy transfer; ligand binding; gel filtration; cross-linking.

INTRODUCTION

Recent studies indicate that UCP2 may catalyze a significant inducible proton conductance in mammalian mitochondria (Echtay *et al*., 2002) and cells (Krauss *et al*., 2002), although it does not appear to contribute to the basal proton conductance (Couplan *et al.*, 2002; Stuart *et al.*, 2001). Regulating this superoxide-inducible conductance may have important cellular consequences, such as controlling insulin secretion (Zhang *et al.*, 2001) and oxidative damage (Arsenijevic *et al.*, 2000; Echtay *et al.*, 2002; Gong *et al.*, 2000). The extent to which UCP2 is recruited likely depends on how strongly the protein binds inhibitory cytosolic nucleotides, and the intracellular conditions (e.g., pH, Mg^{2+}) that may influence this interaction.

To study UCP2–nucleotide interactions, we developed a purified, soluble preparation using a bacterial expression system (Jekabsons *et al.*, 2002). This approach circumvented the technical difficulties of purifying UCP2 from mammalian mitochondria where only limited amounts of the protein are present compared to UCP1 (Pecqueur *et al.*, 2001). We found that inclusion body human UCP2 bound purine and pyrimidine nucleoside triphosphates with approximately 2–5 μM affinity (Jekabsons *et al.*, 2002). Additionally, Mant-modified nucleotides appeared to be convenient probes to monitor

---

[1] Medical Research Council, Dunn Human Nutrition Unit, Wellcome Trust/MRC Building, Hills Road, Cambridge CB2 2XY, United Kingdom.

[2] Present address: Buck Institute for Age Research, 8001 Redwood Blvd., Novato, California 94945.

[3] To whom correspondence should be addressed; e-mail: mjekabsons@ buckinstitute.org.

Key to abbreviation: UCP, uncoupling protein; Mant, *N*-methylanthraniloyl; DMA, dimethylanthranilate; λ_{ex}, excitation wavelength; λ_{em}, emission wavelength; FRET, fluorescence resonance energy transfer; MWCO, molecular weight cutoff.

nucleotide binding by fluorescence resonance energy transfer (Jekabsons *et al.*, 2002).

Although inclusion body UCP2 assumed a nucleotide-binding conformation when treated with $C_{12}E_9$ detergent and hydroxyapatite (Jekabsons *et al.*, 2002), refolding membrane proteins into a "native," homogeneous conformation is often difficult because many different parameters and variables influence protein dynamics. To assess the extent of inclusion body UCP2 refolding, we (a) further tested the utility of Mant-modified nucleotides as valid probes for monitoring UCP2 binding events; (b) more accurately quantified the affinity for [8-^{14}C] ATP and [8-^{14}C] ADP; (c) quantified the stoichiometry of this binding; (d) determined the effects of pH and Mg^{2+} on the apparent affinity for ATP; and (e) determined the physical state of this preparation using a combination of gel filtration, cross-linking, and ultracentrifugation experiments. On the basis of previous work with inclusion body UCP2 (Jekabsons *et al.*, 2002) and UCP1 isolated from brown adipose tissue (Klingenberg, 1988, Klingenberg and Appel, 1989, Lin and Klingenberg, 1980, 1982), several explicit hypotheses were tested in this study. First, we hypothesized that the fluorescence signal obtained with Mant-modified nucleotides is a combination of specific binding to UCP2 and Mant-dependent binding to "nonspecific" sites; this hypothesis developed from the finding that Mant-nucleotide fluorescence with UCP2 was best explained by the presence of two independent binding sites (Jekabsons *et al.*, 2002). Previous competition experiments indicated that UCP2 prefers ATP over ADP as ligand (Jekabsons *et al.*, 2002); consequently, we sought to further test the hypothesis that UCP2 has a greater affinity for ATP than for ADP. Third, we hypothesized that our method of refolding inclusion body UCP2 results in the formation of dimers and that each dimer binds one nucleotide; this hypothesis stems from brown adipose tissue UCP1 experiments indicating that this mitochondrial carrier forms dimers (Klingenberg and Appel, 1989; Lin *et al.*, 1980) and binds one nucleotide per dimer (Lin and Klingenberg, 1980, 1982). Our fourth hypothesis that UCP2 affinity for ATP is reduced with increasing pH and with Mg^{2+} was based on previous work indicating UCP1 binds Mg^{2+}-free nucleotides in a pH-sensitive manner (Klingenberg, 1988).

MATERIALS AND METHODS

UCP2 Preparation

Human UCP2 expression, purification, and refolding from bacterial inclusion bodies was performed (Jekabsons *et al.*, 2002).

FRET Measurements

UCP2 was diluted to 90 μg/mL in 20 mM MOPS, 0.1 mM EDTA, pH 6.8 (the standard assay buffer) at 10°C and titrated with either Mant-ATP or DMA using $\lambda_{ex} = 280$ nm, $\lambda_{em} = 433$ nm, 1.5 nm slit width.

Assessing Mant-ATP and DMA Stoichiometry

UCP2 was incubated in standard assay buffer for 1 h on ice with varying concentrations of either Mant-ATP or DMA. The incubations were transferred to 10-kDa centrifugal filtration devices and centrifuged at $12,500 \times g$ for 15–20 min at 4°C. This centrifugation typically filtered approximately 400 μL from a 1000 μL starting volume. Fluorescence of the resulting protein-free filtrate was determined using $\lambda_{ex} = 355$ nm, $\lambda_{em} = 433$ nm for DMA or 443 nm for Mant-ATP, 1.5 nm slit width. Fluorescent probe bound to UCP2 was calculated by comparing this fluorescence to a set of 19 standards that was also centrifuged through filtration devices. Additionally, the remaining volume retained above the centrifugal filter (the retentate) was collected and FRET fluorescence was determined using $\lambda_{ex} = 280$ nm, $\lambda_{em} = 433$ nm, 1.5 nm slit width.

[8-^{14}C] ATP and [8-^{14}C] ADP Binding by Dowex

UCP2 (22.5 μg) was incubated in 250 μL standard assay buffer with [8-^{14}C] ATP or [8-^{14}C] ADP on ice for 1 h. One hundred and seventy microliters of aliquots were rapidly pressure-filtered through 40 mg water-washed Dowex 1 × 8 (chloride form, 200–400 mesh) columns into scintillation vials (Klingenberg, 1988). Columns were washed twice with 300 μL of water. Filtrate [8-^{14}C] ATP or [8-^{14}C] ADP content was determined by liquid scintillation counting. Bound nucleotide was calculated by subtracting filtrate counts of no protein controls from filtrate counts of UCP2 samples.

[8-^{14}C] ATP and [8-^{14}C] ADP Binding by Centrifugal Filtration

UCP2 (45 μg) was incubated in 500 μL standard assay buffer as with Dowex method. Samples were transferred to 10-kDa centrifugal filtration devices and centrifuged at $12,500 \times g$ for 11 min at 4°C. The [8-^{14}C] ATP or [8-^{14}C] ADP content of the filtrate (volume typically 120–150 μL) was determined by liquid scintillation counting. For some experiments the standard assay buffer was modified by changing to pH 8.0 or adding $MgCl_2$ to 2 mM.

Gel Filtration Chromatography

Hundred microliters UCP2 (230–280 μg protein) was loaded on a Superdex 200 HR 10/30 column equilibrated at 4°C with 20 mM MOPS, 120 mM Na_2SO_4, 0.2% $C_{12}E_9$, 10% glycerol, pH 6.8. Flow rate was 0.2 mL/min and effluent was monitored for absorbance at 230 nm. Fractions (0.37 mL) were collected, assayed for protein, and analyzed by SDS-PAGE. Column was calibrated to determine relative molecular weight of UCP2 using ferritin, aldolase, serum albumin, ovalbumin, and chymotrypsinogen A.

Cross-Linking With Cu^{2+}-Phenanthroline

Experiments were conducted essentially as reported in (Klingenberg and Appel, 1989, Kobashi, 1968). Briefly, 50 μL UCP2 was incubated for 5–10 min on ice with gentle stream of O_2 followed by 10 μL addition of $CuSO_4$ and 1, 10 phenanthroline to final concentrations of 0.25 and 1.3 mM, respectively. Reactions were incubated under a gentle stream of O_2 for a further 30–40 min then stopped by 10 μL addition of EDTA and N-ethylmaleimide to 5 and 2 mM, respectively. Aliquots were added to SDS-PAGE-loading buffer with or without mercaptoethanol and electrophoresed for 50 min at 200 V through 10% acrylamide resolving mini-gels. Quantitation of each band on the dried gels was assessed by densitometry using NIH Image software.

UCP2 Ultracentrifugation

UCP2, either concentrated or diluted to 90 μg/mL in standard assay buffer, was centrifuged at $80,000 \times g$ for 30 min at 4°C. Supernatant aliquots were assayed for protein content in parallel with control samples not centrifuged.

Protein Assay

UCP2 protein was quantified using bicinchoninic acid (BCA) protein assay with BSA as standard. Protein determination by this method was validated by independently determining the concentration by absorbance at 276–282 nm using UCP2 extinction coefficients (values of 26750, 26600, 26115, 25460, and 24400 M^{-1} cm^{-1} for 276, 278, 279, 280, and 282 nm, respectively, determined for human UCP2 sequence from ExPASy molecular biology server: www.expasy.ch). For this, 50 μL

concentrated UCP2 was diluted in 950 μL 5 mM MOPS, 3% SDS, pH 7.2, and absorbance determined at 276, 278, 279, 280, and 282 nm. The protein concentration by BCA assay was within 10% of that determined by absorbance.

Nonlinear Least-Squares Regression Analysis

Dissociation constants and stoichiometry were calculated using either a one- or two-site binding model as previously described (Jekabsons *et al.*, 2002).

RESULTS

Recently, Mant-tagged nucleotides were shown to exhibit enhanced fluorescence by FRET with human UCP2 prepared from bacterial inclusion bodies (Jekabsons *et al.*, 2002). To further investigate the validity of these modified nucleotides as fluorescent probes for monitoring nucleotide binding to UCP2, Mant-ATP titrations were compared with that of DMA (Fig. 1). DMA is the Mant fluorescent group covalently linked to a methyl group rather than a nucleotide and thus served as control for any potential binding due to the Mant group alone. As previously found
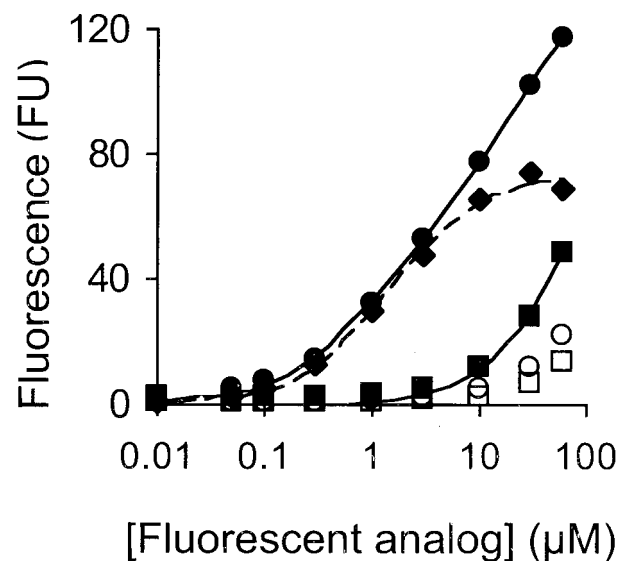

Fig. 1. Mant-ATP and DMA titration of UCP2. 90 μg/mL UCP2 (filled symbols) or 0.2% $C_{12}E_9$ (open symbols) in 20 mM MOPS, 0.1 mM EDTA, pH 6.8 was titrated at 10°C with either Mant-ATP ($\bullet$, $\circ$) or DMA ($\blacksquare$, $\square$). Fluorescence was recorded using λ_{ex} =280 nm, λ_{em} = 433 nm. At each concentration, DMA fluorescence was subtracted from Mant-ATP fluorescence to generate a net titration ($\blacklozenge$). Curves were fit to the data by nonlinear regression using either a two-site ($\bullet$) or one-site ($\blacksquare$, $\blacklozenge$) model of ligand binding.

(Jekabsons *et al.*, 2002), a two independent binding site model best fit the Mant-ATP fluorescence titration. This model yielded a high affinity site with $K_{d1} = 0.9\ \mu M$, fluorescence$_{max}$ = 55 FU and a lower affinity site with $K_{d2} = 23.0\ \mu M$, fluorescence$_{max}$ =87 FU (Fig. 1). A one-site model fit to the DMA titration yielded $K_d = 112\ \mu M$, fluorescence$_{max}$ =137 FU. Subtracting DMA from Mant-ATP fluorescence produced a single-site binding model with $K_d = 1.5\ \mu M$ and fluorescence$_{max}$ = 74 FU.

To assess binding stoichiometry, free-Mant-ATP concentration was determined after incubation with UCP2 for 60 min. Fluorescence of the protein-free centrifugal filtrate was calibrated to that of a standard curve, and the concentration difference used to calculate bound Mant-ATP. From 0.6–4.2 μM total concentration of added probe, UCP2-bound Mant-ATP with $K_d = 0.35 \pm 0.03\ \mu M$ and $B_{max} = 2.1 \pm 0.3$ mol/mol dimer (Fig. 2(A)). Using less than 0.6 μM total Mant-ATP, the free concentration was below the limit of detection; above 4.2 μM total Mant-ATP, bound nucleotide could not be determined due to UCP2 denaturation during the centrifugation step that separates free from bound nucleotide. This concentration-dependent denaturation is illustrated in Fig. 2(B). After UCP2 incubation with Mant-ATP for 60 min, the mixture was centrifuged through filtration devices for approximately 15 min at $12,500 \times g$ to obtain sufficient protein-free filtrate for fluorescence determination. Fluorescence of the reaction retained above the filter (the retentate), determined by FRET, increased continuously to 4.2 μM total Mant-ATP, after which it dropped rapidly to background levels. This drop in fluorescence was associated with visible white precipitates in the samples. For comparison with fluorescence experiments where stoichiometry was not determined (Fig. 1, and Fig. 2(B) open circles), the retentate fluorescence data in Fig. 2(B) was plotted as a function of total, rather than free, Mant-ATP concentration. Single-site nonlinear regression of this data indicated $K_d = 1.7 \pm 0.4\ \mu M$ and fluorescence$_{max}$ = 64 ± 15 FU. If correctly plotted as a function of free Mant-ATP, this curve would be shifted to the left with $K_d = 0.5\ \mu M$.

In separate experiments, FRET fluorescence of the same UCP2 preparations was determined by 0.01–60 μM serial Mant-ATP titrations without centrifugation (Fig. (2B)). Unlike the stoichiometry experiments where the samples were centrifuged, fluorescence continued to increase up to 60 μM total added Mant-ATP, the highest concentration used. Within 0.6–4.2 μM range, fluorescence of these titrations was virtually identical to the FRET retentate samples. This further suggests that UCP2 did not denature during centrifugation with 0.6–4.2 μM Mant-ATP. Two-site analysis of the combined fluorescence data
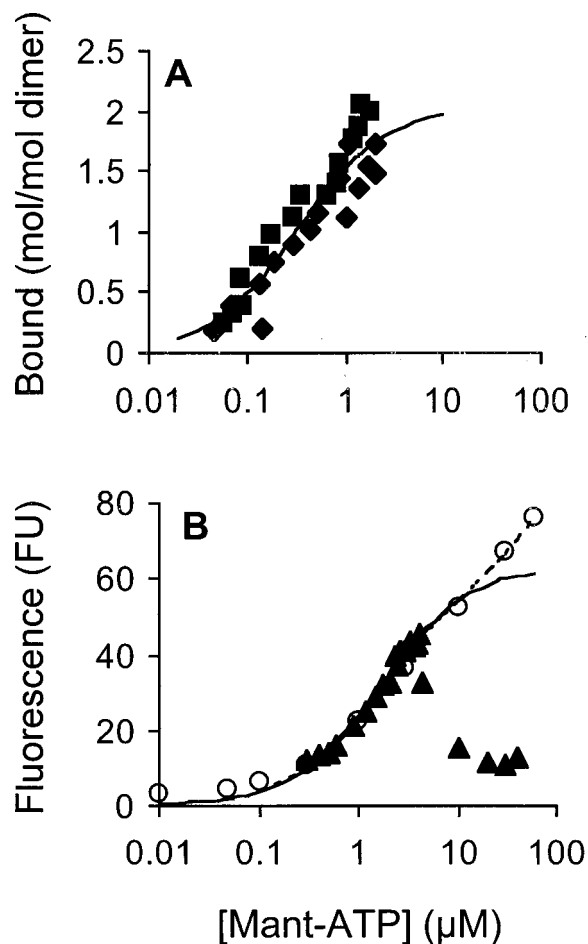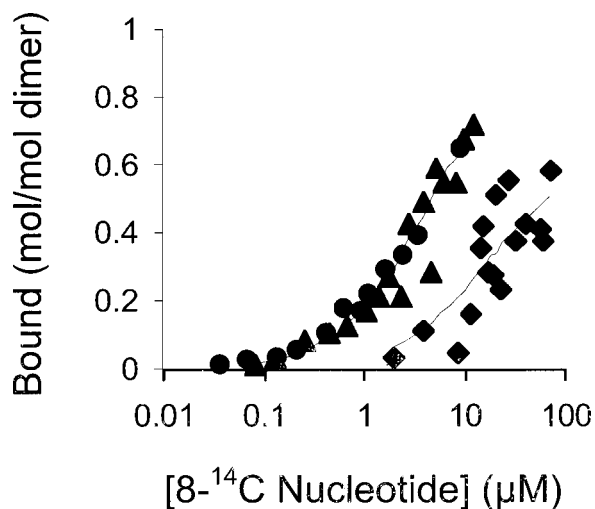

Fig. 2. Stoichiometry of Mant-ATP binding to UCP2 (A) and the corresponding fluorescence (B) associated with this binding. A. Two independent UCP2 preparations (■, ♦) were incubated for 60 min on ice in the standard assay buffer with different concentrations of Mant-ATP. Samples were transferred to 10 kDa MWCO centrifugal filtration devices and centrifuged at $12,500 \times g$ for approximately 15 min at 4°C. This centrifugation typically yielded 400–500 μL filtrate volumes from 1000 μL starting volume. The protein-free filtrate fluorescence was determined using $\lambda_{ex} = 355$ nm, $\lambda_{em} = 443$ nm. Free Mant-ATP was calculated from a 19-point standard curve, and plotted against the resulting bound nucleotide. Curve is best fit least squares nonlinear regression using a single-class binding site model. B. Immediately after centrifugation, fluorescence of the volume not filtered was determined using $\lambda_{ex} = 280$ nm, $\lambda_{em} = 433$ nm and plotted as a function of total Mant-ATP added (▲). For clarity, data are presented as mean of two experiments. For comparison, fluorescence data from separate experiments on the same UCP2 preparations are shown (O). In these experiments, fluorescence was determined using $\lambda_{ex} = 280$ nm, $\lambda_{em} = 433$nm as UCP2 was titrated with increasing concentrations of Mant-ATP at 10°C over 10 min as described in Fig. 1. Solid line is single-site model fit to (▲), omitting those points where fluorescence declines with increasing Mant-ATP. Dashed line is two-site model fit to the combined data set, again omitting those points from (▲) where fluorescence declines.

(Fig. (2B)) produced $K_{d1} = 1.4$ μM, fluorescence$_{max1}$ = 56 FU, and $K_{d2} = 92$ μM, fluorescence$_{max}2 = 54$ FU. The high affinity site of this analysis agrees well with the single-site model from Fig. 1 where DMA fluorescence was subtracted from Mant-ATP fluorescence. The low affinity site of this analysis agrees well with the DMA single-site model (Fig. 1).

The affinity and stoichiometry of UCP2 for [8-^{14}C] ATP and [8-^{14}C] ADP were determined using both centrifugal filtration and dowex chromatography (Fig. 3, Table I). Dissociation constants determined by single-site nonlinear regression were 4–5 μM for ATP and 16–18 μM for ADP. Affinity for ATP was unaffected by increasing pH to 8.0. Addition of 2 mM MgCl$_2$ reduced the apparent ATP affinity to 53 μM (Table I). With the assay conditions used (pH 6.8, 0.1 mM EDTA, 2 mM MgCl$_2$, and approximately 30 mM Na$^+$), Mg^{2+}-free ATP concentrations were calculated using ATP-binding constants for H$^+$, Mg^{2+}, Na$^+$, and EDTA-binding constants for H$^+$ and Mg^{2+}. Nonlinear regression with these values indicated UCP2 affinity for unchelated ATP was 3.1 μM.

UCP2 exhibited a maximum binding capacity of one nucleotide per dimer when the single-site analysis was carried out using nucleotide concentrations ranging from 0.1–12 μM (Fig. 3). Above 12 μM, measured binding increased well beyond one nucleotide per dimer, and the

Table I. UCP2 Dissociation Constants and Binding Stoichiometry for ATP and ADP

	[8-^{14}C] ATP		[8-^{14}C] ADP	
	K_d (μM)	B$_{max}$ (per dimer)	K_d (μM)	B$_{max}$ (per dimer)
Dowex				
pH 6.8	5.3 ± 1.5 (2)	0.9 ± 0.2 (2)	16 (1)	0.8 (1)
Filtration				
pH 6.8	4.4 ± 1.2 (2)	0.9 ± 0.1 (2)	18 (1)	0.6 (1)
+2 mM MgCl$_2$	53 (1)	1.3 (1)	nd	nd
pH 8.0	5.8 ± 3.4 (3)	0.9 ± 0.5 (3)	nd	nd

Note. UCP2 was incubated for 70 min on ice with different concentrations of [8-^{14}C] ATP or [8-^{14}C] ADP in the standard assay buffer without or with 2 mM MgCl$_2$ equilibrated to either pH 6.8 or 8.0. This incubation period was sufficient for equilibrium binding conditions to be achieved. Bound nucleotide was determined by either the dowex or centrifugal filtration method. Dissociation constants (K_d) and binding maximum (B$_{max}$) were determined using nonlinear least-squares regression analysis as in Fig. 3. Parentheses indicate the number of independent preparations used. For each condition where more than one preparation was used, data are mean ± SD. nd: not determined.

Fig. 3. UCP2 binding to [8-^{14}C] ATP and [8-^{14}C] ADP. UCP2 was incubated for 70 min on ice in the standard assay buffer with different concentrations of either [8-^{14}C] ATP (●, ▲) or [8-^{14}C] ADP (◆). Samples were transferred to 10-kDa MWCO centrifugal filtration devices and centrifuged for 11 min at 4°C. Radiolabeled nucleotide content of filtrate samples was determined by liquid scintillation counting. Curves are best fit nonlinear regression analysis using a single receptor class model.

associated Scatchard plots (not shown) became nonlinear. Because these data indicated the presence of a second high capacity, low affinity class of "nonspecific" sites, nonlinear regression analysis of [8-^{14}C] data was restricted to relatively low nucleotide concentrations. In one UCP2 preparation where [8-^{14}C] ATP binding was measured using 25 different concentrations ranging from 0.05–50 μM by centrifugal filtration, the data were sufficient for a two-independent site nonlinear regression analysis that yielded $K_{d1} = 2.1$ μM, $B_{max1} = 0.4$ mol/mol dimer, and $K_{d2} = 76$ μM, B$_{max2} = 4.8$ mol/mol dimer. Thus, an extensive analysis was required to confidently resolve [8-^{14}C] ATP binding to this preparation.
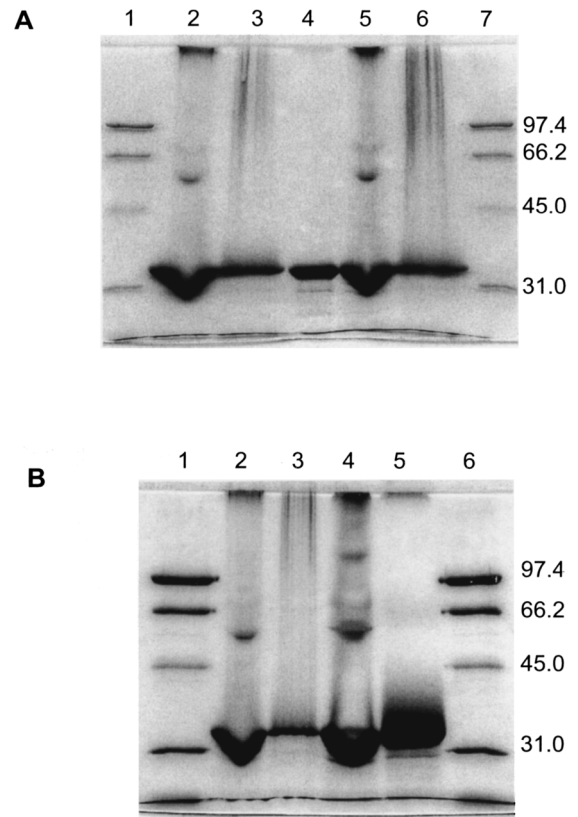
One nucleotide bound per dimer indicated that either inclusion body UCP2 spontaneously formed dimers (or higher polymers) during the refolding protocol, or that this stoichiometry was an artifact of 50% denatured monomers. To distinguish between these possibilities, the oligomeric state of two independent UCP2 preparations was assessed by gel filtration chromatography (Fig. (4) (A) and (B)). Under the conditions used, 64 ± 7% of loaded protein was recovered. The primary peak, constituting 77 ± 8% (mean ± SD, $n = 2$) of recovered protein, eluted with a relative molecular weight of 197 ± 3 kDa. A secondary peak, constituting 18 ± 9% of recovered protein, eluted in the column void volume, indicating aggregated protein. As can be seen, the amount of aggregates in these two preps was quite different; this variability could be due to differences between preparations or gel filtration runs. A minor third peak with an estimated relative molecular
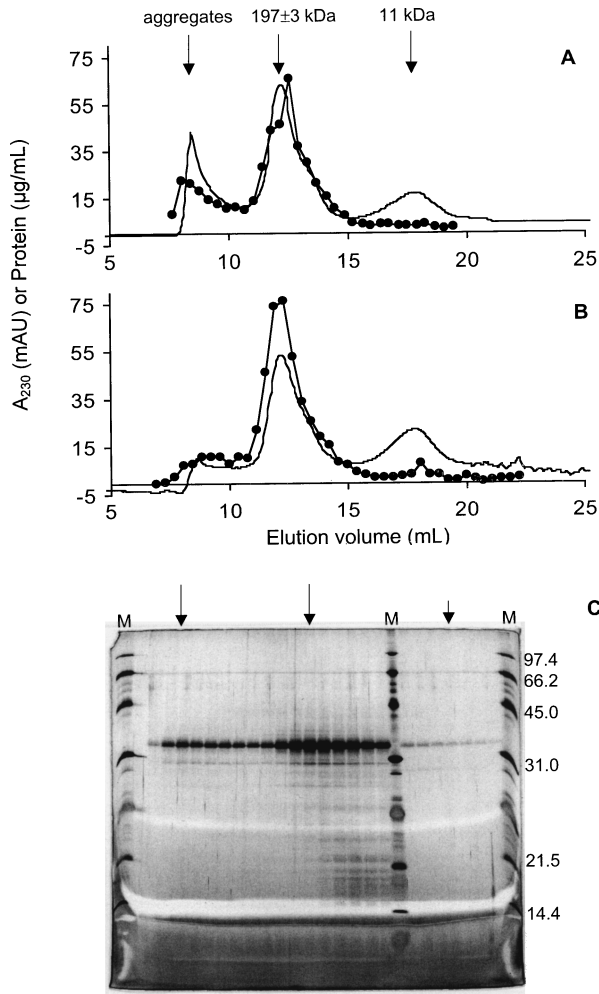
Fig. 4. Gel filtration chromatography of hydroxyapatite-treated inclusion body UCP2. 100 μL of two independent UCP2 preparations (A, B) was run at 0.2 mL/min on a Superdex 200 HR 10/30 gel filtration column and the effluent monitored for absorbance at 230 nm (A_{230}; smoothed lines with no symbols). Relative molecular weights (mean $\pm$ SD of A and B chromatograms) of the peaks eluting outside column void volume are at top of figure. Fractions (0.37 mL) were collected, assayed for protein content by BCA detection ($\bullet$), and 12 μL of each fraction visualized by silver stain on 15% SDS-PAGE gels (C). Molecular weight markers are indicated M, with masses in kilo Dalton indicated at right of gel. Arrows on gel correspond to peaks observed on the chromatogram of (B).

Fig. 5. SDS-PAGE of UCP2 after Cu^{2+}-phenanthroline cross-linking reaction. Two independent UCP2 preparations (A, B) were incubated with Cu^{2+} and 1, 10 phenanthroline under a gentle stream of O_2 for 30–40 min as described in Methods section. Twenty microgramms of protein added to loading buffer without or with mercaptoethanol was electrophoresed through 10% acrylamide and Coomassie stained. A. lanes: 1, 7. molecular weight markers (in kDa indicated at right); 2, 5. two separate cross-link reactions of the same UCP2 preparation in mercaptoethanol-free loading buffer; 3, 6. the same reactions with mercaptoethanol included in the loading buffer; 4. UCP2 not incubated with Cu^{2+}-phenanthroline. B. lanes: 1, 6. molecular weight markers; 2, 3. cross-link reactions without and with, respectively, mercaptoethanol included in loading buffer; 4, 5. crosslink reactions without and with, respectively, mercaptoethanol where UCP2 was first incubated for 10 min with final concentration of 4% SDS.

weight of 11 kDa constituted $5 \pm 1\%$ of recovered protein. SDS-PAGE analysis indicated that both 197 kDa and aggregate peaks were primarily UCP2 (Fig. 4(C)).

Copper-phenanthroline disulfide cross-linking reaction was used to further investigate the oligomeric state of UCP2 (Fig. 5). Most protein electrophoresed as UCP2 33-kDa monomers after reaction with Cu^{2+}-phenanthroline. However, two cross-linked protein bands were clearly visible. One band did not penetrate the

10% acrylamide gel and was considered protein aggregates. The second band migrated with a relative molecular weight of 56.0 ± 1.2 kDa (mean $\pm$ SD, $n = 2$). A third, faint cross-linked product consistently occurred and had a relative molecular weight of 73.0 ± 0.6 kDa. Densitometry indicated that the proportion of protein staining as aggregate, 73.0 kDa, 56.0 kDa, and 33 kDa bands was 19 ± 2, 1 ± 0, 6 ± 1, and $74 \pm 2\%$, respectively. A cross-linked "protein ladder" (bands running at 257, 136, 72.6, 59.2, and 31.4 kDa) was observed when SDS was added to 4% prior to initiating the reaction (Fig. 5(B) lane 4).

	Supernatant protein remaining (%)	Supernatant [8-^{14}4C] ATP binding remaining (%)
Concentrated UCP2	74 ± 5	45
Diluted UCP2	82 ± 11	nd

Note. Final concentrated preparation (2.0–2.3 mg/mL) or UCP2 diluted to 90 μg/mL in the standard assay buffer was centrifuged at 80,000 × g for 30 min at 4°C. Supernatant aliquots were taken for protein assay (mean ± SD; $n = 2$) or [8-^{14}C] ATP binding (mean of duplicates from a single preparation using 1.78 μM [8-^{14}C] ATP). Control samples not centrifuged were run in parallel and data expressed as percentage of these values; nd: not determind.

To independently quantify the amount of UCP2 in aggregate form, samples were centrifuged at 80,000 × g for 30 min, 4°C (Table II). Pelleted protein was considered as high molecular weight aggregates while protein remaining in the supernatant was considered as monodisperse UCP2. Approximately 25% of protein pelleted upon centrifugation, consistent with gel filtration estimate that aggregated protein constiuted 18% of total eluted protein (Fig. 4). The proportion of aggregated protein did not change when diluted to 90 μg/mL in the standard assay buffer used throughout this study. Although 75–80% UCP2 remained as monodisperse protein, there was approximately 50% less [8-^{14}C] ATP binding after 80,000 × g centrifugation ($n = 1$, Table II), indicating that aggregates had significant nucleotide-binding capacity.

DISCUSSION

We recently found that sarkosyl-solubilized inclusion body UCP2 refolds when treated with $C_{12}E_9$ detergent and hydroxyapatite. The conclusion that UCP2 at least partially refolded into functional form was based on enhanced fluorescence of Mant-nucleotides by FRET and on [8-^{14}C] ATP competition experiments with unmodified nucleotides (Jekabsons *et al.*, 2002). As detailed in the Introduction section, the current studies were designed to test specific hypotheses, all of which served to further our understanding of using hydroxyapatite-treated inclusion bodies as a means to study uncoupling protein 2 function.

Fluorescently tagged compounds are useful for monitoring protein–ligand interactions if the protein maintains a specificity for the ligand rather than simply having an affinity for the fluorescent tag. Previously, we found that FRET fluorescence of Mant-modified nucleotides with UCP2 may result from two independent binding sites (Jekabsons *et al.*, 2002). This indicated the possibility

that inclusion body UCP2 contained a nucleotide binding site able to accept Mant-modified nucleotides and a separate, independent site interacting with the Mant group (which we refer to as DMA). The current results show that UCP2 does interact with DMA in a manner that produces FRET fluorescence (Fig. 1). Substracting FRET fluorescence obtained with DMA from that obtained with Mant-ATP removes the "nonspecific" signal because of the Mant portion of the modified nucleotide. The "specific" fluorescence was best explained by a single class of binding sites having 1.5 μM affinity. This dissociation constant was similar to 0.9 μM (this study) and 0.46 μM (previous study; Jekabsons *et al.*, 2002) high-affinity dissociation constants determined for non-DMA corrected Mant-ATP fluorescence using a two-site model. UCP2 affinity for DMA alone (approximately 112 μM, Fig. 1) was similar to the 23 μM (Fig. 1) or 92 μM (Fig. 2(B)) low-affinity Mant-ATP site determined by two-site analysis. While these data are not sufficient to accurately determine DMA affinity, they clearly allow us to conclude that Mant-nucleotide fluorescence signals obtained by FRET were a combination of specific, nucleotide-related interaction, and nonspecific, fluorescent-tag related interaction with UCP2. Since tryptophan and tyrosine residues participate in energy transfer, the nonspecific DMA-related fluorescence may occur at a UCP2 epitope different from the nucleotide binding site. Steric constraints at the nucleotide binding site is one argument that the two fluorescence-associated sites are distinct. In any case, DMA serves as an essential control for potential fluorescence unrelated to ligand-specific binding.

Stoichiometry experiments indicated the high-affinity site had 0.35 μM K_d with 2 mol Mant-ATP bound per mol dimer UCP2. Retentate FRET fluorescence from these experiments plotted as a function of total Mant-ATP concentration (Fig. 2(B), filled triangles) was identical to that obtained from separate acute titration experiments and indicated a 1.7-μM high-affinity site. However, we emphasize that plotting fluorescence as a function of total Mant-ATP concentration underestimated the affinity ($K_d = 1.7$ μM) by approximately threefold compared to a correct analysis using free-Mant-ATP concentrations ($K_d = 0.5$ μM). To summarize, UCP2 titrated with Mant-ATP produced FRET fluorescence best explained by two independent binding sites, with $K_d = 0.9 - 1.7$ μM for the high-affinity site and 23–92 μM for the low-affinity site using total Mant-ATP concentrations for the analysis. DMA titrations indicated 112 μM K_d, consistent with a low-affinity binding site for the fluorescent tag. Determination of free Mant-ATP in conjunction with FRET fluorescence revised the high-affinity site K_d to 0.35–0.5 μM. Thus, with appropriate DMA controls, Mant-ATP is a

useful probe for monitoring nucleotide binding to purified inclusion body UCP2.

Radiolabeled nucleotide binding indicated UCP2 affinity for ATP and ADP was 4–5 and 16–18 μM, respectively, similar to our previous 2 and 23 μM estimates using competition experiments (Jekabsons *et al.*, 2002). Compared to Mant-ATP, this order of magnitude lower affinity indicates that UCP2 hydrophobic interaction with the fluorescent tag is substantial. This is similar to UCP1 interaction with Dansyl-modified nucleotides (Huang and Klingenberg, 1995). The apparent affinity reduction for ATP with physiological concentrations of $MgCl_2$ was remozved after analysis with calculated non-chelated free-ATP concentrations. Thus, UCP2 binds Mg-tree nucleotides. In terms of physiological regulation of UCP2 one might ask if the presence of millimolar cellular magnesium removes enough "ligand-competent" ATP and ADP by chelation to reduce the free concentration sufficiently close to the dissociation constants measured in this study. Total cell ATP concentrations are 2–10 mM and total Mg content 15–20 mM, with 5–10% existing as free Mg^{2+} (Headrick *et al.*, 1998; Romani and Scarpa, 2000; Schwenke *et al.*, 1981). Using these values, we calculate that unchelated ATP could be 50–700 μM, but with the concentration more likely 100–300 μM. This concentration range, 25-75-fold above our experimentally determined K_d for ATP, suggests that virtually the entire UCP2 pool is inhibited by ATP. A substantial reduction (10-fold or more) in free ATP would be necessary to activate UCP2 by displacing the nucleotide. This seems unlikely since ATP levels are very stable under most circumstances. With 100–200-fold less total ADP than ATP (Huang and Klingenberg, 1995; Lawson and Veech, 1979; Portman *et al.*, 1997; Ronner *et al.*, 2001), unchelated ADP would be about 4–40 μM, which encompasses our measured 18 μM K_d for ADP. Even with an extreme 10-fold reduction in unchelated ATP to activate UCP2, unchelated ADP levels would increase sufficiently to offset any activation that would occur from ATP reduction. Thus, it seems that UCP2 affinity for ADP is not sufficiently different from ATP to be physiologically meaningful and that UCP2 recruitment could only occur by the action of an activator to overcome nucleotide control. Such a scenario has been proposed for UCP1, with fatty acids liberated from triglyceride stores by hormone sensitive lipase as the activator (Locke *et al.*, 1982), but it is not widely accepted. Superoxide stimulates UCP2 in isolated mitochondria, but the $K_{0.5}$ for inhibition of this effect by GDP is about 17 μM (Echtay *et al.*, 2002), similar to the K_d for GDP binding to UCP2 in the absence of superoxide (Jekabsons *et al.*, 2002), suggesting that superoxide cannot activate nucleotide-inhibitied UCP2.

UCP1 nucleotide affinity decreases with increasing pH (Klingenberg, 1988). This pH effect does not seem to be physiologically meaningful because brown adipocyte cytosolic pH rises only about 0.1 pH unit after exposure to norepinephrine (Lee *et al.*, 1994). Such a pH rise would reduce UCP1 affinity for ATP from about 3–6 μM (Klingenberg, 1988). A 6-μM dissociation constant is more than adequate to maintain UCP1 inhibition given cytosolic unchelated ATP of 100–300 μM. In this respect, the pH-dependence of nucleotide binding to UCP1 may be of interest only as a means of understanding mechanisms of nucleotide interaction with the protein. Refolded UCP2 did not exhibit a pH-dependent change in affinity for ATP, suggesting that the mechanism of nucleotide interaction with UCP2 is different than UCP1. Alternatively, these data could indicate that this UCP2 preparation is not in an entirely refolded conformation since UCP1 residues that impart pH-sensitivity (Echtay, 1997, 2000; Klingenberg *et al.*, 1995; Klingenberg and Huang, 1999,) are well conserved in UCP2, and nucleotide inhibition of superoxide-activated UCP2 in mitochondria may be strongly pH dependent (Echtay *et al.*, 2002).

We found that UCP2 bound one [8-^{14}C] ATP or [8-^{14}C] ADP per dimer. This is identical to the nucleotide binding stoichiometry of UCP1 isolated from brown adipose tissue (Lin and Klingenberg, 1980, 1982) and suggests that the minimum functional unit of UCP2 is dimeric. Our finding that UCP2-bound 2 mol Mant-ATP per mol dimer may indicate that these modified nucleotides interact with UCP2 in a different manner than their unmodified counterparts. Alternatively, the comparison between the standards and UCP2 samples in these experiments may be inappropriate due to inherent filtrate differences that resulted in altered Mant-ATP emissions (e.g., presence of quenching agent in UCP2 but not standards filtrate samples).

When solubilized, the seven transmembrane helix protein bacteriorhodopsin binds 119 mol $C_{12}E_8$ detergent per mol monomer (Moller and le Maire, 1993). Using this stoichiometry for the six transmembrane helix protein UCP2 in $C_{12}E_9$, monomer molecular weight would be 103 kDa. By gel filtration, we found the primary UCP2 peak to be 197 kDa, consistent with a dimeric or polymeric structure. Additionally, UCP1 solubilized from brown adipose tissue with Triton X-100 exhibited 180 kDa relative molecular weight by gel filtration, which corresponded to a dimer after estimation of the Triton associated with UCP1 (Lin *et al.*, 1980). Cross-linked protein running as 56 kDa by SDS-PAGE further supports the hypothesis that the 197 kDa gel filtration peak is dimeric UCP2. The faint 73 kDa cross-linked species likely represents trimers, either present in the monodisperse population or induced

by cross-linking. Alternatively, the 73-kDa protein may be completely linearized UCP2 dimers whereas the 56-kDa species may be dimers resistant to complete denaturation by SDS-PAGE. The quantitative difference in dimers by gel filtration (77%) and cross-linking (6%) probably reflects the inefficiency of the Cu^{2+}-phenanthroline reaction. This inefficiency may be due to spatial orientation and/or accessibility of the sulfhydryl groups within UCP2. By the same reaction, less than half of native UCP1 is cross-linked (Klingenberg and Appel, 1989). Since cross-linking likely depends on sulfhydryl group accessibility and orientation, the different pattern observed without vs. with 4% SDS added indicates that this treatment changed the UCP2 conformational state. Because cross-linking with SDS yielded as much Coomassie-stained dimer as without SDS, we cannot formally rule out the possibility that dimers seen without SDS result from collision of monomers. However, since gel filtration indicated the presence of quaternary structure (i.e., UCP2 monomers ordered into a higher oligomeric state, excluding aggregates) the cross-linked dimers could reflect the 197-kDa gel filtration species rather than collision of monomers. Our tentative conclusion that inclusion body UCP2 may form dimers agrees with studies indicating dimeric structures for less related mitochondrial carriers, such as the phosphate, adenine nucleotide, and oxoglutarate carriers (Klingenberg *et al.*, 1995; Palmisano *et al.*, 1998; Schoers *et al.*, 1998).

Aggregates determined by Cu^{2+}-phenanthroline cross-linking amounted to 19% of total Coomassie-stained protein by SDS-PAGE, which agrees with 18% determined by gel filtration and 25% determined by ultracentrifugation. We speculate that cross-linking of aggregates was quantitatively similar to gel filtration and ultracentrifugation because of closer orientation and/or greater exposure of sulfhydryl groups within the aggregated protein. Importantly, we found that after aggregated protein was removed by ultracentrifugation, [8-^{14}C] ATP binding per mg protein was reduced by about 50%. Since aggregates accounted for 50% of bound nucleotide, binding stoichiometry of the monodisperse protein could be 1 per tetramer rather than 1 per dimer. The hydroxyapatite method used to select refolded UCP2 should completely adsorb aggregated and denatured protein; consequently, aggregate formation either occurred during the concentration step of hydroxyapatite column fractions, or upon freeze/thawing of the concentrated protein. In either case, nucleotide binding to aggregates should be considered nonspecific binding. Further binding experiments using $80,000 \times g$ treated protein are necessary to determine nucleotide interactions with the monodisperse protein without complications arising from the presence of aggregates.

In summary, FRET fluorescence of Mant-ATP is a valid means to assess nucleotide binding to purified inclusion body UCP2 when used in conjunction with DMA controls. The utility of these probes to detect nucleotide binding to UCP2 in isolated mitochondria remains to be determined. UCP2 binds Mg-free nucleotides and exhibits a 4-fold greater affinity for ATP than ADP at pH 6.8. Given prevailing intracellular conditions, this affinity difference does not seem to be physiologically important for regulating UCP2. ATP did not bind to UCP2 in a pH-sensitive manner. Approximately 75–80% of this inclusion body UCP2 preparation exists as monodisperse protein having an apparent molecular weight of 197 kDa, consistent with a dimeric or polymeric structure. Approximately 6% of Cu^{2+}-phenanthroline-treated UCP2 electrophoresed as 56-kDa-dimeric protein by SDS-PAGE, while 75% remained as monomers; this further indicates the possibility of dimeric UCP2. One radiolabeled nucleotide was bound per dimer or perhaps per higher polymer, suggesting that the functional form of UCP2 is not a monomer.

ACKNOWLEDGMENTS

REFERENCES

Arsenijevic, D., Onuma, H., Pecqueur, C., Raimbault, S., Manning, B. S., Miroux, B., Couplan, E., Alves-Guerra, M. C., Goubern, M., Surwit, R., Bouillaud, F., Richard, D., Collins, S., and Ricquier, D. (2000). *Nat. Genet.* **26**, 435–439.

Couplan, E., Del Mar Gonzalez-Barroso, M., Alves-Guerra, M. C., Ricquier, D., Goubern, M., and Bouillaud, F. (2002). *J. Biol. Chem.* **277**, 26268–26275.

Echtay, K. S., Bienengraeber, M., and Klingenberg, M. (1997). *Biochemistry* **36**, 8253–8260.

Echtay, K. S., Roussel, D., St-Pierre, J., Jekabsons, M. B., Cadenas, S., Stuart, J. A., Harper, J. A., Roebuck, S. J., Morrison, A., Pickering, S., Clapham, J. C., and Brand, M. D. (2002). *Nature* **415**, 96–99.

Echtay, K. S., Winkler, E., Bienengraeber, M., and Klingenberg, M. (2000). *Biochemistry* **39**, 3311–3317.

Gong, D. W., Monemdjou, S., Gavrilova, O., Leon, L. R., Marcus-Samuels, B., Chou, C. J., Everett, C., Kozak, L. P., Li, C., Deng, C., Harper, M. E., and Reitman, M. L. (2000). *J. Biol. Chem.* **275**, 16251–16257.

Headrick, J. P., McKirdy, J. C., and Willis, R. J. (1998). *Am. J. Physiol.* **275**, H917–H929.

Huang, S. G., and Klingenberg, M. (1995). *Biochemistry* **34**, 349–360.

Jekabsons, M. B., Echtay, K. S., and Brand, M. D. (2002). *Biochem. J.* **366**, 565–571.

Klingenberg, M. (1988). *Biochemistry* **27**, 781–791.

Klingenberg, M., and Appel, M. (1989). *Eur. J. Biochem.* **180**, 123–131.

Klingenberg, M., Echtay, K. S., Bienengraeber, M., Winkler, E., and Huang, S. G. (1999). *Int. J. Obes. Relat. Metab. Disord.* (Suppl. 6), S24–S29.

Klingenberg, M., and Huang, S. G. (1999). *Biochim. Biophys. Acta* **1415**, 271–296.

Klingenberg, M., Winkler, E., and Huang, S. G. (1995). *Methods Enzymol.* **260**, 369–389.

Kobashi, K. (1968). *Biochim. Biophys. Acta* **158**, 239–245.

Krauss, S., Zhang, C. Y., and Lowell, B. B. (2002), *Proc. Natl. Acad. Sci. U.S.A.* **99**, 118–122.

Lawson, J. W., and Veech, R. L. (1979). *J. Biol. Chem.* **254**, 6528–6537.

Lee, S. C., Hamilton, J. S., Trammell, T., Horwitz, B. A., and Pappone, P. A. (1994). *Am. J. Physiol.* **267**, C349–C356.

Lin, C. S., Hackenberg, H., and Klingenberg, M. (1980). *FEBS Lett.* **113**, 304–306.

Lin, C. S., and Klingenberg, M. (1980). *FEBS Lett.* **113**, 299–303.

Lin, C. S., and Klingenberg, M. (1982). *Biochemistry* **21**, 2950–2956.

Locke, R. M., Rial, E., and Nicholls, D. G. (1982). *Eur. J. Biochem.* **129**, 381–387.

Moller, J. V., and le Maire, M. (1993). *J. Biol. Chem.* **268**, 18659–18672.

Palmisano, A., Zara, V., Honlinger, A., Vozza, A., Dekker, P. J., Pfanner, N., and Palmieri, F. (1998). *Biochem. J.* **333**, 151–158.

Pecqueur, C., Alves-Guerra, M. C., Gelly, C., Levi-Meyrueis, C., Couplan, E., Collins, S., Ricquier, D., Bouillaud, F., and Miroux, B. (2001). *J. Biol. Chem.* **276**, 8705–8712.

Portman, M. A., Xiao, Y., Song, Y., and Ning, X. H. (1997). *Am. J. Physiol.* **273**, H1977–H1983.

Romani, A. M., and Scarpa, A. (2000). *Front. Biosci.* **5**, D720–D734.

Ronner, P., Naumann, C. M., and Friel, E. (2001). *Diabetes* **50**, 291–300.

Schoroers, A., Burkovski, A., Wohlrab, H., and Kramer, R. (1998). *J. Biol. Chem.* **273**, 14269–14276.

Schwenke, W. D., Soboll, S., Seitz, H. J., and Sies, H. (1981). *Biochem. J.* **200**, 405–408.

Stuart, J. A., Harper, J. A., Brindle, K. M., Jekabsons, M. B., and Brand, M. D. (2001). *J. Biol. Chem.* **276**, 18633–18639.

Zhang, C. Y., Baffy, G., Perret, P., Krauss, S., Peroni, O., Grujic, D., Hagen, T., Vidal-Puig, A. J., Boss, O., Kim, Y. B., Zheng, X. X., Wheeler, M. B., Shulman, G. I., Chan, C. B., and Lowell, B. B. (2001). *Cell* **105**, 745–755.